ELSEVIER

Polymer 42 (2001) 10013–10019

polymer

www.elsevier.com/locate/polymer

PP/clay nanocomposites prepared by grafting-melt intercalation

Xiaohui Liu[a,b,*], Qiuju Wu[a]

[a]Department of Materials and Manufacturing Engineering, Division of Polymer Engineering, Luleå University of Technology, Luleå SE 97187, Sweden
[b]State Key Laboratory of Engineering Plastics, Institute of Chemistry, Chinese Academy of Sciences, Beijing 100080, China

Received 23 May 2001; received in revised form 24 July 2001; accepted 31 July 2001

Abstract

Polypropylene (PP)/clay nanocomposites (PPCN) were prepared via grafting-melt compounding by using a new kind of co-intercalation organophilic clay which had a larger interlayer spacing than the ordinarily organophilic clay only modified by alkyl ammonium. One of the co-intercalation monomers was unsaturated so it could tether on the PP backbone by virtue of a grafting reaction. The larger interlayer spacing and strong interaction caused by grafting can improve the dispersion effect of silicate layers in the PP matrix, which was confirmed by X-ray diffraction (XRD) and transmission electron microscopy (TEM). The mechanical properties of PPCN were improved with the addition of clay. The incorporation of silicate layers also gave rise to a considerable increase of the storage modulus (stiffness) and a decrease of the tan δ value, demonstrating the reinforcing effect of clay on the PP matrix. Besides, the glass transition temperature (T_g) of PPCN decreased in the presence of the silicate layers. The addition of clay did not change the crystal structure of PP, however silicate layers acted as nucleating agents for the crystallization of PP. © 2001 Elsevier Science Ltd. All rights reserved.

Keywords: PP/clay nanocomposite; Organophilic clay; Dispersion

1. Introduction

In recent years, organic-inorganic nanometer composites have attracted great interest from researchers since they frequently exhibit unexpected hybrid properties synergistically derived from two components. One of the most promising composites systems would be hybrids based on organic polymers and inorganic clay minerals consisting of layered silicates [1–25]. Since the synthesized Polyamide 6/clay nanocomposites were first demonstrated by a group at the Toyota research center in Japan [10–12], much research effort has explored the improvement in performance as a few weight percent of nano-silicate was added to polymer.

The most commonly used clay is the smectite group mineral such as montmorillonite (MMT), which belongs to the general family of 2:1 layered silicates. Their structures consist of two fused silica tetrahedral sheets sandwiching an edge-shared octahedral sheet of either aluminium or magnesium hydroxide. The silicate layers are coupled through relatively weak dipolar and van der Waals forces. The Na^+ or Ca^{2+} residing in the interlayers can be replaced by organic cations such as alkylammonium ions via an ion-exchange reaction to render the hydrophilic layered silicate organophilic [1]. In all of the methods to prepare the polymer/clay nanocomposites, the most versatile and environmentally benign approach is based on direct polymer melt intercalation.

Polypropylene (PP) is one of the most widely used polyolefin polymers, it does not include any polar group in its backbone, but silicate layers even modified by nonpolar long alkyl groups are polar and incompatible with polyolefin [26–28]. Up to now there are two major methods to prepare a PP/clay nanocomposite (PPCN): (1) polar functional oligomer as a comptabilizer [26–28]. Polyolefin oligomers with polar telechelic OH groups (PO–OH) and maleic anhydride modified PP oligomers are used in this method. The driving force of the intercalation originates from the strong hydrogen bonding between the OH groups of the PO–OH or maleic anhydride group (or COOH group generated from the hydrolysis of the maleic group) and the oxygen groups of the silicates. The interlayer spacing of the clay increases, and the interaction of the layers should be weakened. The intercalated clay with the oligomers contacts PP under a strong shear field. If the miscibility of the oligomers with PP is good enough to disperse at the molecular level, the exfoliation of the intercalated clay should take place [26]. (2) Clay is pre-dispersed in the polymer compatible to PP [29,30]. In this method, organophilic clay is dispersed in solvent at first, unsaturated monomers are polymerized

* Corresponding author. Tel.: +46-920-91770; fax: +46-920-91084.
E-mail address: xiaohui.liu@mb.luth.se (X. Liu).

0032-3861/01/$ - see front matter © 2001 Elsevier Science Ltd. All rights reserved.
PII: S0032-3861(01)00561-4

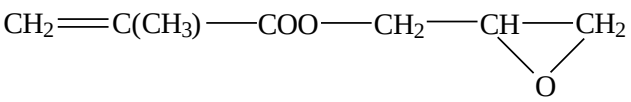

Fig. 1. Chemical structure of epoxypropyl methacrylate.

between the silicate layers in solvent environment to expand the interlayer spacing and form the compatible polymer to PP. After blending the polymer containing intercalated clay with PP, the silicate layers can be dispersed well in the PP matrix.

In this study, we suggest a new method to prepare PPCN. A kind of co-intercalation organophilic clay is used which has a larger interlayer spacing than the ordinarily organophilic clay only modified by alkyl ammonium; one of the co-intercalation monomers is unsaturated so that it could tether on the PP backbone by virtue of a grafting reaction. The larger interlayer spacing and strong interaction caused by the grafting reaction can improve the dispersion effect of silicate layers in the PP matrix. The corresponding properties of the resulting nanocomposites were investigated.

2. Experiment

2.1. Materials

PP, 2401, used in this study was manufactured by Yanshan Petrol and Chem. Co. The cation exchange capacity (CEC) of Na-montmorillonite used in this article was 80 meq/100 g. The water content was about 7 wt% at original state (TGA method). The particle size was less then 20 μm.

The organophilic clay was prepared as the reference via ion exchange reaction in water using alkylammonium. 100 g Na-montmorillonite was dispersed into 5000 ml of hot water using homogenizer. 30 g hexadecyl trimethyl ammonium bromide was dissolved into hot water. It was poured into the Na-montmorillonite–water solution under vigorous stirring for 30 min to yield white precipitates. The precipitates were collected and washed by hot water three times, and then the precipitates were ground to 20 μm after thoroughly drying in a vacuum oven. This organophilic clay was designated as C16-MMT.

The co-intercalation organophilic clay was prepared as follows: 130 g C16-MMT and 20 g epoxypropyl methacrylate (its chemical structure shown in Fig. 1) were mixed in a Haake Reocorder 40 mixer for 1 h. Before mixing with clay, the initiator of grafting reaction, dibenzoyl peroxide (BPO), and donor agent were solved in epoxypropyl methacrylate. The obtained product was designated as EM-MMT.

The interlayer distances of the above organophilic clays and Na-montmorillonite were measured by X-ray diffraction (XRD) of the powder specimens.

2.2. Preparation of PP/clay nanocomposites

A twin-screw extruder was used for the preparation of the nanocomposites. The temperature of the extruder was maintained at 180, 190, 200 and 190°C from hopper to die, respectively. The screw speed was maintained at 180 rpm. The dried pellets of the nanocomposite were injection-molded into test pieces for mechanical tests and measurements of the dynamic moduli. The temperature of the cylinders was 200°C and that of the mold was 30°C.

2.3. Characterization

The thin films (400 μm) of the nanocomposites were prepared by pressing at 200°C for the XRD measurements to evaluate the dispersibilities of the silicate layers in the PP matrix. XRD was performed at room temperature by a Ragaku Model D/max-2B diffractometer; the X-ray beam was nickel-filtered CuKα_1 ($\lambda = 0.1504$ nm) radiation operated at 40 kV and 30 mA; corresponding data were collected from 1.5 to 40° at a scanning rate of 2°/min. TEM observations were performed for the thin sections of the injection-molded samples by a Hitachi H-800 TEM using an acceleration voltage of 200 kV.

Prior to testing, all specimens were dried in a vacuum oven at 80°C for 6 h. The tensile testing was carried out on a universal tensile tester (INSTRON 8501), the notched Izod impact strength was measured with CS-137D-167 (Custom Scientific Instruments Inc.) according to the respective standards.

The dynamic mechanical analysis was performed using a dynamic mechanical analyzer (Perkin–Elmer DMA-7). The testing was carried out in three-point bending mode at a vibration frequency of 1 Hz in a temperature range from −50 to 150°C at a heating rate of 5°C/min in nitrogen atmosphere.

DSC analyses were carried out using a Perkin Elmer DSC-7 differential scanning calorimeter thermal analyzer. About 10 mg of the polymer sample was weighed very accurately in the aluminium DSC pan and placed in the DSC cell. It was heated from 30 to 200°C at a rate of 10°C/min under nitrogen atmosphere. The sample was kept for 10 min at this temperature to eliminate the heat history before cooling at 10°C/min. The thermograms corresponding to the heating and cooling cycles are shown in Fig. 11.

3. Results and discussion

3.1. The intercalation effect of EM-MMT

Fig. 2 presents the XRD patterns of E-MMT, C16-MMT and Na-montmorillonite, respectively. Na-montmorillonite has a characteristic diffraction peak corresponding to the (001) plane at 1.24 nm. C16-MMT shows a 1.96 nm basal space in XRD pattern. The basal space of EM-MMT is

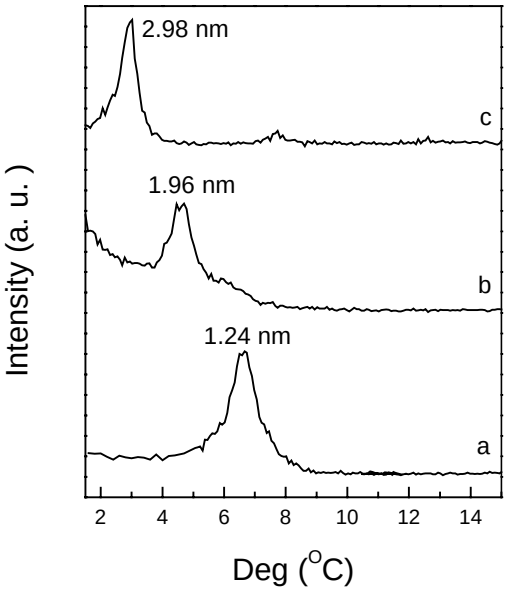

Fig. 2. XRD patterns of (a) Na-montmorillonite; (b) C16-MMT; (C) EM-MMT.

2.98 nm as shown in Fig. 2. Comparing the 2.98 nm d_{001} value of EM-MMT with the 1.96 nm d_{001} value of C16-MMT and 1.24 nm of Na-montmorillonite, the obviously larger layer distance demonstrates the advantage of co-intercalation organophilic clay EM-MMT.

The alkylammonium ion exchange enables the conversion of the hydrophilic interior clay surface to hydrophobic and increases the layer distance as well, like the condition of C16-MMT which has been used widely in nanocomposite. Based on this organophilc environment, epoxypropyl methacrylate can then be swollen into the clay galleries easily to increase the layer distance further. For this method applied with EM-MMT we use the term co-intercalation.

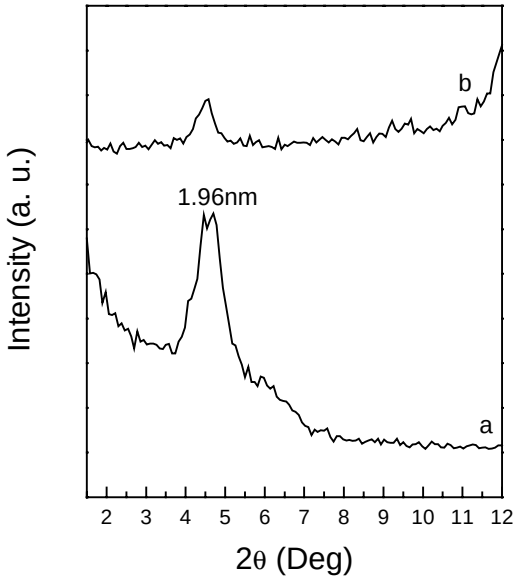

Fig. 3. XRD patterns of (a) C16-MMT; (b) mixture of PP and C16-MMT.

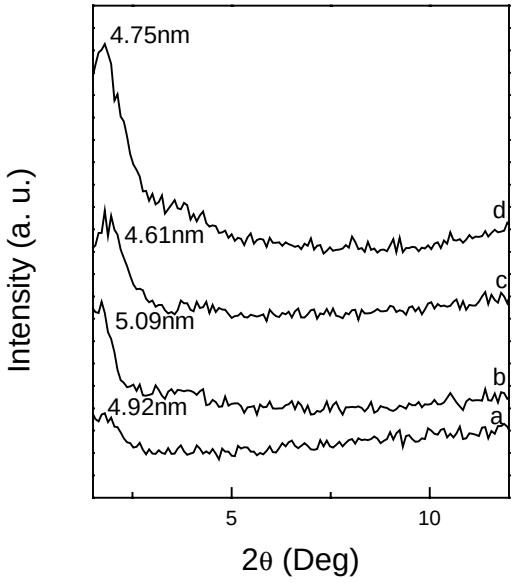

Fig. 4. XRD patterns of (a) PPCN1; (b) PPCN3; (c) PPCN5; (d) PPCN7.

The advantage of this method is to increase the basal spacing of clay and bring the functional groups into the galleries.

3.2. The dispersibility of EM-MMT in PP matrix

The direct evidence of the intercalation is provided by the XRD patterns of the obtained hybrids. The XRD pattern of the mixture of C16-MMT (5 wt%) with PP is presented in Fig. 3. The result clearly shows that the (001) plane peak of the clay does not shift to lower angle at all, which indicates that PP does not intercalate into C16-MMT. As suggested by Kawasumi et al. [26], PP does not include any polar groups in its backbone, and the silicate layers of clay, even modified by nonpolar long alkyl groups, are polar and incompatible with polyolefin.

Fig. 4 shows the XRD patterns of PP nanocomposites compounding with EM-MMT in different loading, The PP nanocomposite containing 1 wt% EM-MMT is abbreviated as PPCN1, similarly, the nanocomposites having 3, 5, and 7 wt% EM-MMT are abbreviated as PPCN3, PPCN5, and PPCN7, respectively. As shown in figure, PPCN1 has a 4.92 nm basal spacing; with increasing clay content, the basal spacing of PPCN3 increases up to 5.09 nm; more clay contents cause slight reduce in basal spacing, PPCN5 is 4.61 nm and PPCN7 is 4.75 nm. Compared with ordinarily organophilic clay C16-MMT, a better intercalation effect is observed when using co-intercalation clay EM-MMT. From the basal spacing observed in PP nanocomposites with EM-MMT, PPCN are a kind of intercalated nanocomposite.

The dispersibility of EM-MMT in the PP matrix is also confirmed by TEM shown in Fig. 5, where the dark lines are the intersection of the silicate layers of 1 nm thickness. Similar to the unintercalated layered silicate; individual

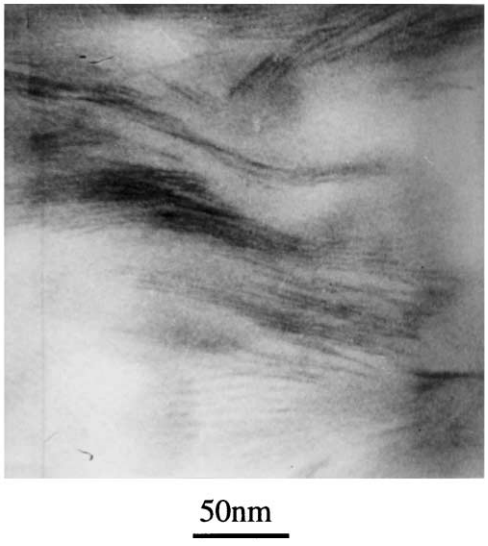

Fig. 5. TEM image of PPCN5.

layers of silicate are visible as regions of alternating dark and light bands. The only different is the expansion of layer distance to accommodate the intercalated polymer. In this case, one can see the silicate layers still maintain the ordered stacking in the PP matrix while the layer distance ranges from 3 to 5 nm. Some silicate layers are dispersed and delaminated in the PP matrix.

Vaia et al. [25] suggested that the confinement of the polymer inside the interlayers results in a decrease in the overall entropy of the polymer chains. At the same time, the entropic penalty of polymer confinement may be compensated by the increased conformational freedom of the tethered surfactant chains as the layers separate. But this mean-field model also indicates that the entropy associated with the aliphatic chains only increases until the tethered chains are fully extended. For the system of clay only treated with hexadecyl trimethyl ammonium bromide, a ca. 3.5 nm basal spacing reflects the length of fully extended 16-carbon aliphatic chain [14,16,25]. Further

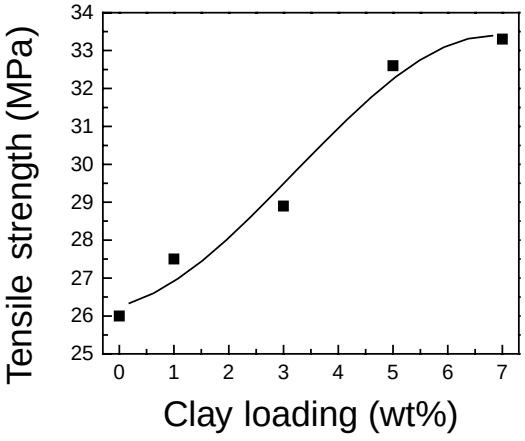

Fig. 6. Effect of clay loading on tensile strength of PPCN.

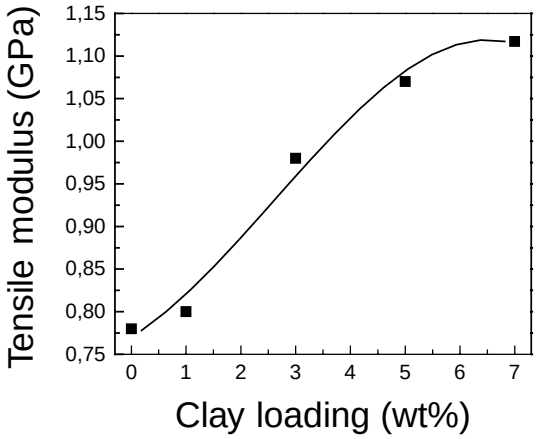

Fig. 7. Effect of clay loading on tensile modulus of PPCN.

layer separation depends on the establishment of very favourable interactions to overcome the continually increasing penalty of polymer confinement, and then the reason why the silicate layers of EM-MMT have better dispersion effect than C16-MMT is self-evident. Firstly, the co-intercalation of epoxypropyl methacrylate increases the interlayer spacing of clay, the interaction of the layers should be weakened; secondly, with the unsaturated double bond, epoxypropyl methacrylate residing inside the galleries of clay can easily graft on the PP backbone under the effect of initiator, such that the reaction heat is another driving force to expand the layer distance.

3.3. Mechanical properties

The mechanical properties of PPCN are measured and summarized in Figs. 6–8. The tensile strength of PPCN increases rapidly with increasing clay content from 0 to 5 wt%, the tensile strength of PPCN5 is 32.7 MPa. But the increasing trend is less when the clay content increases beyond 5 wt%, PPCN7 has a 33.1 MPa tensile strength. 27% improvement in tensile strength is obtained in

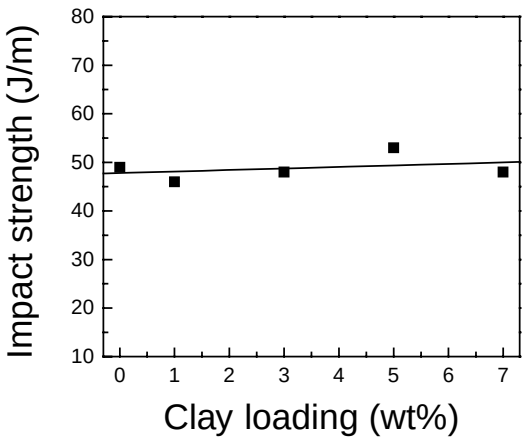

Fig. 8. Effect of clay loading on notched Izod impact strength of PPCN.

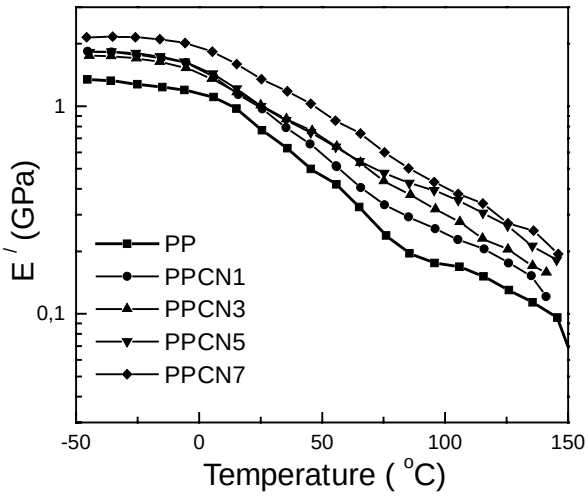

(a)

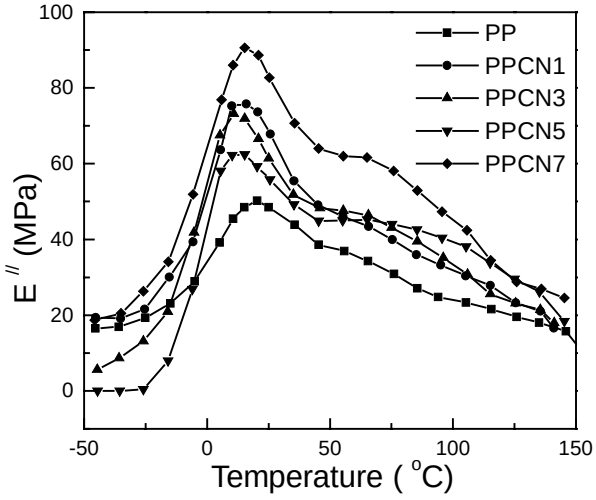

(b)

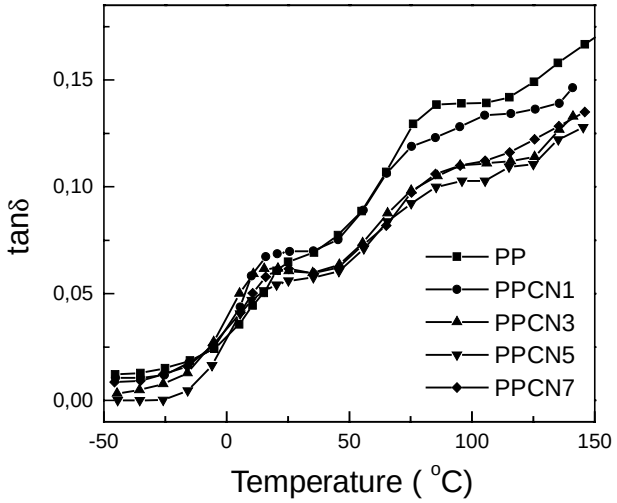

(c)

Fig. 9. Dynamic mechanical spectra ((a) storage modulus E'; (b) loss modulus E''; (c) loss factor tan δ) as a function of temperature for PP and PPCN.

Table 1
Dynamic storage moduli of the samples at various temperatures

	Storage modulus, E', (GPa)				T_g (°C)
	−45°C	25°C	85°C	135°C	
PP	1.35 (1.00)	0.77 (1.00)	0.20 (1.00)	0.11 (1.00)	19.45
PPCN1	1.85 (1.37)	0.97 (1.26)	0.29 (1.45)	0.15 (1.36)	12.54
PPCN3	1.75 (1.30)	1.01 (1.31)	0.37 (1.85)	0.17 (1.55)	10.46
PPCN5	1.82 (1.35)	1.00 (1.30)	0.43 (2.15)	0.21 (1.91)	13.58
PPCN7	2.15 (1.59)	1.35 (1.75)	0.50 (2.50)	0.22 (2.00)	15.79

PPCN7 compared with PP. A similar phenomenon is observed in Fig. 7. While a 42% increase in tensile modulus is obtained in PPCN7. The notched Izod impact strength of PPCN is basically constant within the experimental error in the clay content range of 0–7 wt%.

The nanometeric dispersion of silicate layers in matrix leads to improved modulus and strength. The stiffness of the silicate layers contributes to the presence of immobilized or partially immobilized polymer phases; those phases have been thoroughly discussed by Eisenberg [31]. It is also possible that silicate layer orientation as well as molecular orientation contribute to the observed reinforcement effects. The lower stiffening above 5 wt% clay loading can be attributed to the inevitable aggregation of the layers in high clay content.

3.4. Dynamic mechanical properties

Fig. 9 depicts the dynamic mechanical spectra (dynamic storage modulus E', dynamic loss modulus E'', and loss factor tan δ) as a function of temperature for PP and PPCN. McCrum and colleagues have demonstrated that the tan δ curve of PP exhibits three relaxations localized in the vicinity of −80°C (γ), 100°C (α) and at 10°C (T_g) [32]. The dominant relaxation appeared at ca. 10°C is the glass-rubber relaxation of the amorphous portion of PP. The weak peak appeared as a shoulder at about 100°C is associated with the crystalline regions of PP. In the present work, the study is focused on the temperature range from around T_g up to around T_m, thus the γ relaxation at −80°C is invisible. Some values of E' and T_g at different temperatures are presented in Table 1.

The results show clearly that the addition of clay into PP matrix results in a remarkable increase of stiffness and decrease of tan δ value. The E' curves display an improved rubbery plateau indicating that the addition of clay induces a reinforcement effect. As shown in Table 1, at higher temperature above 80°C, the values of E' of PPCN are two times or higher than that of PP. The reinforcement should increase the thermal-mechanical stability of the material at high temperatures. While a significant decrease is detected for the intensities of two relaxations on tan δ curves of PPCN, only a slight change can be observed for their shapes.

There is one interesting phenomenon. The values of T_g of

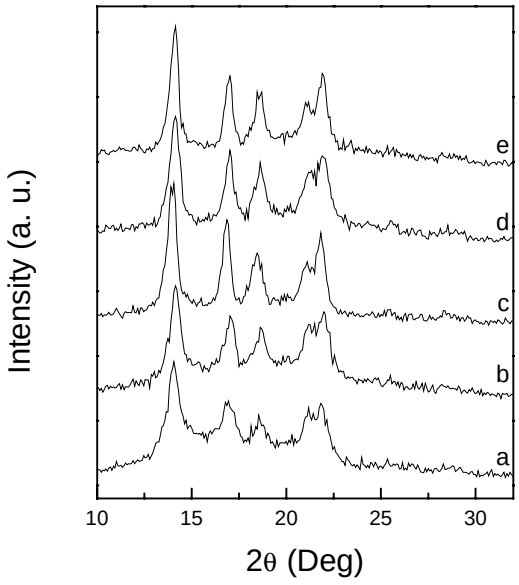

Fig. 10. Crystal structures of (a) PP; (b) PPCN1; (c) PPCN3; (d) PPCN5; (e) PPCN7.

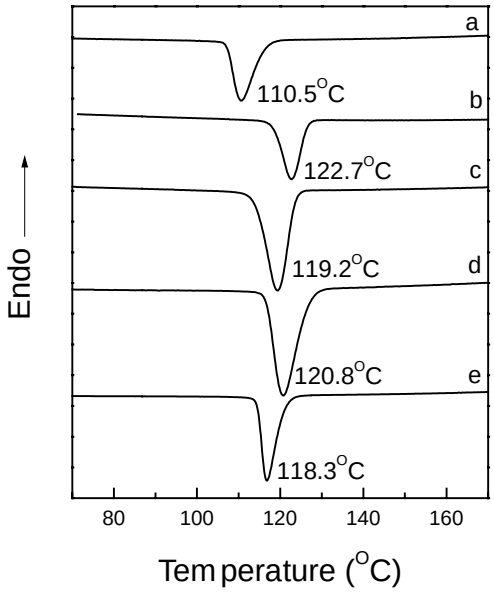

Fig. 11. DSC cooling scan thermograms of (a) PP; (b) PPCN1; (c) PPCN3; (d) PPCN5; (e) PPCN7.

PPCN and PP are presented in Table 1 derived from E'' and tan δ curves. PP has a 19.45°C T_g; 1 wt% clay loading decreases it to 12.54°C; lowest T_g is obtained in PPCN3 at 10.46°C. However, more clay loading does not lower T_g further, in contrast, T_g of PPCN is increasing with increasing clay content when the clay content is above 3 wt%. The mechanism of how the addition of clay affects the T_g of PPCN needs to be studied further.

3.5. Crystal structure and crystallization behavior of PPCN

Fig. 10 shows the XRD patterns of PP and PPCN. The result indicates that there is no obvious difference between PP and PPCN. The addition of clay does not affect the crystal structure of the PP matrix in this case. Fig. 11 presents the DSC cooling scan thermograms of PP and PPCN. The crystallization peak temperature of PP is 110.5°C; while 1 wt% clay addition increases this temperature up to 122.7°C; though slight decrease, that of PPCN3 is 119.2°C; at higher clay contents, the crystallization peak temperatures maintain around 120°C. The DSC results clearly show that the addition of a small amount of clay into the PP matrix results in an increase of crystallization temperature of the polymer matrix. The effect observed can be explained by the assumption that the silicate layers act as efficient nucleating agents for the crystallization of PP matrix.

4. Conclusion

A new kind of co-intercalation organophilic clay was used in this study which had a larger interlayer spacing than organophilic clay modified by alkyl ammonium; one of the co-intercalation monomers was unsaturated so that it could tether on the PP backbone by a grafting reaction. The larger interlayer spacing and reaction heat caused by grafting can improve the dispersion effect of silicate layers in PP matrix. The mechanical properties of PPCN were improved by the addition of clay. The incorporation of silicate layers also gave rise to a considerable increase of the storage modulus (stiffness) and a decrease of the tan δ value demonstrating the reinforcing effect of clay on the PP matrix. The PP glass transition temperature (T_g) decreased in the presence of the silicate layers. The addition of clay did not change the crystal structure of PP, however it accelerated the crystallization considerably.

References

[1] Whittingham MS, Jacobson AE. Intercalation chemistry. New York: Academic Press, 1982.
[2] Theng BKG. The chemistry of clay organic reactions. London: Adam Hilger, 1974.
[3] Giannelis EP. Adv Mater 1993;8:29.
[4] Krishnamoorti R, Giannelis EP. Macromolecules 1997;30:4097.
[5] Vaia RA, Giannelis EP. Macromolecules 1997;30:8000.
[6] Balazs AC, Singh C, Zhulina E. Macromolecules 1998;31:8370.
[7] Lyatskaya Y, Balazs AC. Macromolecules 1998;31:6676.
[8] Novak BM. Adv Mater 1993;6:422.
[9] Lu S, Melo MM, Zhao J, Pearce EM, Kwei TK. Macromolecules 1995;28:4908.
[10] Usuki A, Kawasumi M, Kojima Y, Fukushima Y, Okada A, Kurauchi T, Kamigaito O. J Mater Res 1993;8:1179.
[11] Kojima Y, Usuki A, Kawasumi M, Kojima Y, Fukushima Y, Okada A, Kurauchi T, Kamigaito O. J Mater Res 1993;8:1185.
[12] Kojima Y, Usuki A, Kawasumi M, Kojima Y, Fukushima Y, Okada A, Kurauchi T, Kamigaito O. J Polym Sci, A Polym Chem 1993;31:1755.
[13] Wang MS, Pinnavaia TJ. Chem Mater 1994;6:468.
[14] Lan T, Pinnavaia TJ. Chem Mater 1994;6:2216.
[15] Kelly P, Akelah A, Qutubuddin S, Moet A. J Mater Sci 1994;29:2274.
[16] Vaia RA, Isii H, Giannelis EP. Chem Mater 1993;5:1694.
[17] Moet A, Akelah A. Mater Lett 1993;18:97.

[18] Messersmith PB, Giannelis EP. J Polym Sci, A Polym Chem 1995;33:1047.
[19] Biasci L, Aglietto M, Ruggeri G, Ciardelli F. Polymer 1994;35:3296.
[20] Ogawa M. Chem Mater 1996;8:1347.
[21] Ruiz-Hitzky E, Aranda P, Casal B, Galvan JC. Adv Mater 1995;7:180.
[22] Vaia RA, Vasudevan S, Krawiec W, Scanlon LG, Giannelis EP. Adv Mater 1995;7:154.
[23] Oriakhi CO, Nafshan RL, Lerner MW. MRS Bull 1996;31:1513.
[24] Friedlander HZ, Frink CR. Polym Lett 1964;2:475.
[25] Vaia RA, Jandt KD, Kramer EJ, Giannalis EP. Macromolecules 1995;28:8080.
[26] Kawasumi M, Hasegawa N, Kato M, Usuki A, Okada A. Macromolecules 1997;30:6333.
[27] Hasegawa N, Kawasumi M, Kato M, Usuki A, Okada A. J Appl Polym Sci 1998;67:87.
[28] Kato M, Usuki A, Okada A. J Appl Polym Sci 1997;66:1781.
[29] Kurokawa Y, Yasuda H, Kashiwagi M, Oyo A. J Mater Sci Lett 1997;16:1670.
[30] Kurokawa Y, Yasuda H, Oyo A. J Mater Sci Lett 1996;15:1481.
[31] Tsagaropoulos G, Eisenberg A. Macromolecules 1995;28:6067.
[32] McCrum NG, Read BE, Williams G. Anelastic and dielectric effects in polymeric solids. London: Wiley, 1967.